International Dairy Journal 97 (2019) 149–157

Contents lists available at ScienceDirect

International Dairy Journal

journal homepage: www.elsevier.com/locate/idairyj

Thermodynamic and whipping properties of milk fat in whipped cream: A study based on DSC and TD-NMR

Yunna Wang [a], Dongdong Yuan [b], Yang Li [a], Meiling Li [a], Yuru Wang [a], Yan Li [b], Liebing Zhang [a, *]

[a] College of Food Science and Nutritional Engineering, China Agricultural University, Beijing, 100083, China
[b] Beijing Engineering and Technology Research Centre of Food Additives, Beijing Technology and Business University, Beijing, 100048, China

ARTICLE INFO

Article history:
Received 11 January 2019
Received in revised form
21 May 2019
Accepted 25 May 2019
Available online 4 June 2019

ABSTRACT

The correlation between thermodynamic and whipping properties of milk fat when used in recombined dairy cream (RDC) was investigated; thermodynamic behaviour of milk fat and the microstructure of RDC were analysed. Differential scanning calorimetry curves of anhydrous milk fats (AMFs) showed two peaks (7 °C and 15 °C), implying a difference in the crystallisation mechanisms. RDCs whipped at 7 °C demonstrated significantly higher cream overrun, firmness, and shorter optimum whipping time in comparison with these attributes at 15 °C. Additionally, RDC whipped at 7 °C generated bigger milk fat globules and was characterised by less flocculation and fewer broken air bubbles. Comparative analysis of the whipping properties at 7 °C and 4 °C revealed no significant differences. The results suggest that 7 °C is a more suitable temperature than 15 °C at which to whip RDC, and an ideal alternative temperature to that of 4 °C, for lower energy consumption.

1. Introduction

Whipped cream is a popular dairy component in the production of desserts, pastries, cakes and ice creams. It usually comprises 30–35% fat, which is an important contributory factor in the rheological and sensory properties of the final product (Sajedi, Nasirpour, Keramat, & Desobry, 2014). Recombined dairy cream (RDC), produced by recombining anhydrous milk fat (AMF) and milk protein concentrate (MPC), has wide applications in the food industry. One important property of RDC is its capacity to be transformed from an oil-in-water (O/W) emulsion into a triphasic system through whipping. Whipped RDC is a complex system of air bubbles with milk fat globules (MFGs) on the surface, and the MFGs are partially coalesced by the fat crystals that protrude through the globule membrane (Fredrick, Walstra, & Dewettinck, 2010; Hotrum, Stuart, van Vliet, Avino, & van Aken, 2005).

Good quality whipped RDC should have a desirable firmness, a high overrun (OR) and adequate stability, which can be optimised by ensuring an efficient envelopment of the air bubbles by partially coalesced MFGs. Various strategies, most commonly temperature controls, are used to create partial coalescence (Fredrick et al., 2010; Hotrum et al., 2005). Previous studies have shown that temperature significantly influences the properties of crystallised fat (Moens, De Clercq, Verstringe, & Dewettinck, 2015). The state of fat crystals, namely solid fat content (SFC), varies with temperature and affects the stability of emulsions. Increasing temperature leads to partial melting of the fat crystals, during which the three-dimensional crystal network is broken and the remaining fat crystals can move freely and energetically to a more favourable interface (Fredrick et al., 2010). Conversely, decreasing temperature induces growth in the crystals near the interface, resulting in larger crystals that can penetrate further into the aqueous phase, thereby increasing the susceptibility to partial coalescence (Moens, Masum, & Dewettinck, 2016). Therefore, temperature is critical for controlling the physical characteristics of AMF and, thus, the quality of RDC.

Tempering dairy cream at 30 °C can improve its whipping properties by reducing the whipping time and loss of serum, while simultaneously increasing its overrun and firmness (Drelon et al., 2006). Kamath, Huppertz, Houlihan, and Deeth (2008) reported that cream exhibits a high foaming property at 5 °C but no foaming at 25 °C. The viscosity and surface tension of cream decreases with increasing temperature, while the elastic behaviour of whipped cream has been found to increase when tempered at 25 °C due to

* Corresponding author. Tel.: (+86)13901147036.
E-mail address: liebzhang@gmail.com (L. Zhang).

https://doi.org/10.1016/j.idairyj.2019.05.008
0958-6946/

increased connectivity between the MFGs (Drelon et al., 2006). Temperature is, therefore, thought to affect the introduction of air bubbles as well as other physical properties of cream during the whipping process. However, little is known about the precise influences of different temperatures, as these have yet to be evaluated.

In this study, a differential scanning calorimetry (DSC) assay was used to observe the phase transitions of AMFs, during which peaks appeared at temperatures of 7 and 15 °C. These two temperatures were subsequently employed in whipping tests, together with the temperature of 4 °C, which is routinely used in RDC whipping process and storage. Three AMF samples were used to prepare the whipped cream, in which the relationship between thermal behaviour, crystallisation kinetics and whipping properties were studied. On the basis of these results, this study subsequently evaluated the suitability of the three temperatures in the preparation and storage of whipped cream from an industry perspective.

2. Materials and methods

2.1. Materials

One commercial AMF originating in New Zealand (denoted as AMF-A) and two commercial AMFs from China (denoted as AMF-B and AMF-C) were purchased from supermarkets in Beijing. Milk protein concentrate (MPC) containing 72.1% (w/w) protein, 1.4% (w/w) fat, 16.9% (w/w) lactose and 7.46% (w/w) ash, was kindly donated by Cezanne Co., Ltd. (Yinchuan, Ningxia, China). Microcrystalline cellulose (MCC), soybean lecithin and Tween-80 were purchased from Cargill Co. (Beijing, China). All other reagents and solvents were of analytical or chromatographic grade to suit analytical requirements.

The chemical components of the three AMFs are summarised in Table 1. The Fatty acid (FA) species were identified using the retention time of a fatty acid methyl ester (FAME) standard. FAMEs were prepared according to AOCS Official Method Ce 2-668 and subsequently analysed with GC-14B gas chromatography (GC) equipped with a flame ionisation detector (Agilent, CA, USA), and a DB-WAX capillary column (30 m × 0.25 mm × 0.25 μm). The temperature of the injection port and detector were both set at 200 °C. The column was heated to 40 °C, held for 3 min, then programmed at 5 °C min^{-1} to 120 °C. The temperature was then increased to 200 °C at 10 °C min^{-1}, and held for 13 min. FAME peaks were identified by comparing the retention times with those of a standard mixture of FAMEs. The triglycerides (TAGs) were separated using ultra-high performance liquid chromatography (UHPLC) with a Waters 1525 binary pump (Milford, MA, USA). UHPLC was performed on a liquid chromatography (LC) system (I-class ACQUITY UPLC System; Waters) using a BEH C18 column (1.7 μm, 2.1 mm ID × 100 mm; Waters). An API 4500 QTRAP mass spectrometer (AB SCIEX, Framingham, MA, USA) equipped with an electrospray ion source was connected to the UHPLC system for the MS analysis. All experiments were conducted in positive ionisation mode. The peak areas of individual TAGs analysed with the QTRAP 4500 (AB SCIEX) system were collected and used to calculate the concentrations (Meng et al., 2011).

2.2. Production of recombined dairy cream

The three AMFs, namely AMF-A, AMF-B and AMF-C, were used to prepare recombined dairy cream, correspondingly denoted as RDC-A, RDC-B and RDC-C. Briefly, each AMF was heated to 80 °C to ensure complete melting before soybean lecithin and Tween-80 were dissolved into the liquid fat to constitute the oil phase. MPC was dispersed into deionised water and then incubated in a water bath at 45–50 °C with overhead agitation (RW 20.n; IKA Co., Ltd., Guangzhou, Guangdong, China) at 600 rpm for 1 h to ensure complete hydration. MCC was added into the deionised water at 45–50 °C and treated using a rotor-stator mechanical homogeniser (Ningbo Biotechnology Co. Ltd., Ningbo, Zhejiang, China) to impose shearing force at 9000 rpm for 5 min. The prepared oil phase, MPC solution and MCC dispersion were subsequently mixed and homogenised in a two-stage high-pressure homogeniser (APV1000; Shanghai Shen Lu Homogeniser Co. Ltd., Shanghai, China) under 15 MPa during the first stage and 4 MPa during the second stage. The final recombined dairy cream consisted of 36% (w/w) AMF, 2% (w/w) MPC, 0.3% (w/w) MCC, 0.2% (w/w) soybean lecithin and 0.05% (w/w) Tween-80. After homogenisation, the mixtures were sterilised at 121 °C for 7 min and immediately thereafter cooled to room temperature in a water bath. The samples were then stored at 4 °C for 24 h before being subject to measurements and analysis.

2.3. Differential scanning calorimetry

The melting and crystallisation behaviours of the three AMFs were analysed using differential scanning calorimetry (DSC) (TA Instruments, Crawley, Hampshire, UK). Samples (10 μL) were hermetically sealed in alodine-aluminium pans and an empty pan was used as reference. The DSC sample pans were successively subjected to the following thermal treatments: (i) heating to 80 °C to ensure complete melting, (ii) cooling by 5 °C min^{-1} to −15 °C, (iii) holding at −15 °C for 2 min and, finally, (iv) heating by 5 °C min^{-1} to 40 °C. The DSC was calibrated with indium at a heating rate of 5 °C min^{-1}. Nitrogen was used to purge the system. The enthalpy $\triangle H_M$ (J g^{-1}) is determined as the area limited by the melting curve and base line; similarly, the enthalpy $\triangle H_C$ (J g^{-1}) is determined as the area limited by the crystallisation curve and base line (Tomaszewska-Gras, 2013).

2.4. Time domain nuclear magnetic resonance

Following the AOCS Official Method Cd 16b-93, the SFC of the AMF was determined on a time domain nuclear magnetic resonance (TD-NMR) spectrometer (Bruker, Karlsruhe, Baden-Württemberg, Germany). The sample was placed in the NMR tube, melted at 80 °C for 30 min, frozen at −20 °C for 90 min and then maintained at a range of desired temperatures (0, 5, 10, 15, 20, 25, 30, 35 and 40 °C) for 30 min before measurement until an equilibrium temperature is reached (Liu, Meng, Zhang, Shan, & Wang, 2010). Duplicate measurements were conducted.

2.5. Avrami model analysis

Each sample underwent isothermal crystallisation by being, first, held at 80 °C for 30 min to destroy all crystal remains and then immediately transferred to a temperature-controlled water bath. Two different isothermal crystallisation temperatures, 7 °C and 15 °C, were employed. SFC readings were taken at appropriate time intervals. Data obtained were analysed with Origin 8.0 (OriginLab Corporation, Northampton, PE, USA).

Isothermal Avrami kinetics is concerned with the overall crystallisation process, including nucleation and growth (Wang et al., 2011). The Avrami equation is given as [equation (1)]:

$$\ln[-\ln(1-f)] = n \ln t + \ln K \quad (1)$$

in which f is SFC amount at time t during crystallisation; K is crystallisation rate constant; n is the Avrami exponent (a constant); The K and n are calculated from the intercept and slope obtained by plotting *ln[-ln(1-f)]* against *lnt*, respectively. The overall rate of crystallisation is given by equation (2):

$$t_{\frac{1}{2}}^{n} = \frac{\ln 2}{K} \quad (2)$$

where $t_{1/2}$ is the half-time of crystallisation.

2.6. Stability

The stability of the RDCs was measured on a LUMiFuge [LUM (Changzhou) Instruments Co. Ltd, Changzhou, Jiangsu, China]. A freshly prepared sample (1 mL) was added to the bottom of the cell (2 mm disposable polyamide sample cell with a rectangular cross section). The cell was placed horizontally into the instrument after capping the cell. In the measurement process, at preset time intervals, parallel near-infrared (NIR) light scans the sample cell over its entire length, and the transmission as function of distance from the top of the sample cell is recorded (Bigikocin, Mert, & Alpas, 2011; Yuan, Xu, Qi, Zhao, & Gao, 2011). The multi-sample analytical centrifuge used in this study employs space- and time-resolved extinction profiles technology, which allows the measurement of the intensity of transmitted near-infrared light as a function of time and position over the entire sample length without scanning. The following instrument parameters were used for the measurements: rotation of 450 g, time interval of 30 s, temperature at 4, 7 or 15 °C for 2 h, respectively (after being stored at the same temperature for 24 h, respectively) and a light factor of 1.00 (Zhou et al., 2016).

2.7. Particle size distribution observation

The size distribution of the RDC emulsion droplets was determined on a Malvern MasterSizer 3000 (Malvern Instruments Co., Ltd., Malvern, Worcestershire, UK) after RDC samples being stored at 4, 7 and 15 °C for 24 h, respectively. The refractive index, dispersed phase adsorption, and continuous phase refractive index were set to 1.52, 0.1, and 1.33, respectively. The emulsion was diluted in recirculating water until 10–20% obscuration was reached. Each sample was measured in triplicate (Han et al., 2018).

2.8. Whipping properties

2.8.1. Whipping process

Whipping of the RDC was performed immediately after storage at 4, 7 or 15 °C for 24 h. The cream was whipped using a kitchen mixer (AHM-P125A ACA, Zhuhai, Guangdong, China) firstly at 950 rpm for 30 s, and then at 1100 rpm until reaching the optimum whipping time (t_{wh}), when the cream broke away from the mixer and no longer flowed. Whipping experiments were repeated twice for each cream. The overrun and firmness of each whipped sample were determined at 4, 7 and 15 °C, respectively (Fredrick et al., 2013).

2.8.2. Overrun

Overrun (OR) is a measure of the amount of air introduced in whipped cream. According to Fredrick et al. (2013), it can be calculated by comparing the mass of equal volumes of un-whipped and whipped cream [equation (4)]:

$$overrun(\%) = \frac{m1 - m2}{m2} \times 100\% \quad (4)$$

where m_1 is the mass of the un-whipped cream and m_2 is the mass of the whipped cream, which were measured six times after each whipping.

2.8.3. Firmness

Deformation puncture measurements were conducted on a Texture Analyzer TA500 (Lloyd Instruments, London, UK) equipped with an acrylic cylindrical probe (diameter 25 mm, height 35 mm). Puncture tests were performed at a rate of 1 mm s^{-1} over a distance of 20 mm on the surface of the whipped cream. The trigger threshold value for the start of the measurement was set at 0.01 N (Fredrick et al., 2013). The force (N) required to reach this depth (20 mm) is defined as the firmness of the whipped cream.

2.9. Confocal laser scanning microscopy

Confocal laser scanning microscopy (CLSM) was used to observe the microstructure of the RDC. Nile red (NR) (0.02%, w/v, in dimethyl sulfoxide) and fluorescein isothiocyanate (FITC) (0.02%, w/v, in distilled water) were added to the cream just before whipping to label fat and protein compositions, respectively. Whipped cream samples were immediately observed after whipping at temperatures of 4, 7 or 15 °C, at which the observed RDCs were stored correspondingly for 24 h before whipping. The whipping experiments were done in duplicate, as shown in Section 2.7.1.

A Leica inverted microscope DM IRE2 TCS SP2 (Leica Microsystems, Heidelberg, Baden-Württember, Germany) equipped with a 10 × objective was applied to acquire the images. Both FITC and NR were excited by an argon laser light at 488 nm. The fluorescence emitted by the FITC and NR were detected separately in two photomultiplier tubes in wavelength ranges of 500–536 nm and 595–648 nm, respectively (Han et al., 2018).

2.10. Data analysis

All of the tests were conducted in at least duplicate in this study. One-way analysis of variance (one-way ANOVA) was conducted using IBM SPSS 21 (IBM SPSS Inc., Chicago, IL, USA). A difference of $P < 0.05$ was regarded as statistically significant.

3. Results and discussion

3.1. Thermodynamic characteristics

The content and physical state of fat play critical roles in the physicochemical properties of creams (Smith, Go, & Kakuda, 2000). Whipped cream and some other aerated emulsions require SFC content ≥40% to promote partial coalescence. Solidification profiles for the AMFs are illustrated in Fig. 1. The SFC curves of all samples exhibited a similar tendency, namely, the SFC of each sample decreased with increase of crystallisation temperature. The SFC of all AMFs were approximately 45–55% at 7 °C, and were approximately 25–35% at 15 °C. The AMF-A still contained solid fat at nearly 40 °C, which may explain its waxy mouthfeel (Karabulut, Turan, & Ergin, 2004). The AMF-C turned to liquid at 30 °C, suggesting that it would melt completely at body temperature. Indeed, the various kinds of AMFs in this study demonstrated different SFC profiles, possibly due to their different chemical compositions. The AMF-A, for example, contained more long chain short chain FAs (SFAs) and tri-saturated (S3) triacylglycerides (TAGs) compared with the other two AMFs, which resulted in a higher melting point (Table 1). As a result, AMF-A crystallised quickly and had the highest SFC at all temperatures. In contrast, the AMF-C comprised

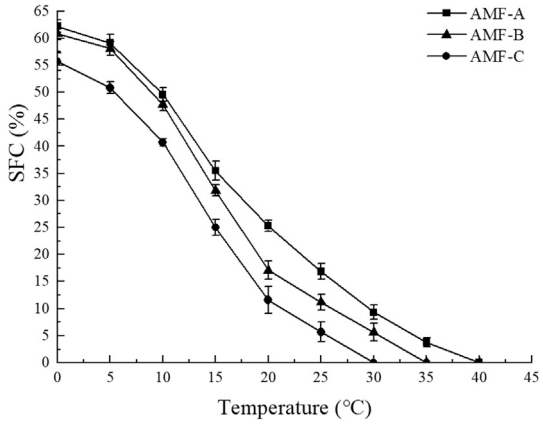

Fig. 1. Solid fat content (SFC) at equilibrium as function of crystallisation temperature for anhydrous milk fats: ■, AMF-A; ▲, AMF-B; ●, AMF-C.

Table 1
Basic chemical compositions of anhydrous milk fats (AMFs).[a]

Component	AMF-A	AMF-B	AMF-C
Fatty acids			
SFA	69.12 ± 2.38[a]	65.23 ± 1.47[b]	63.39 ± 1.23[c]
USFA	30.88 ± 1.05[a]	34.77 ± 1.22[b]	36.61 ± 1.35[c]
Triacylglycerides			
S3	45.83 ± 1.13[a]	43.90 ± 1.27[b]	40.46 ± 1.46[c]
S2U	29.62 ± 1.01[a]	30.03 ± 0.48[a]	29.83 ± 0.13[a]
SU2	20.59 ± 0.78[a]	21.64 ± 1.11[b]	24.24 ± 1.35[c]
U3	3.95 ± 0.03[a]	4.43 ± 0.05[b]	5.48 ± 0.05[c]

[a] Abbreviations are: SFA, saturated fatty acid; USFA, unsaturated fatty acid; S3, tri-saturated; S2U, di-saturated-monounsaturated; SU2, mono-saturated-di-unsaturated; U3, tri-unsaturated. Values are percentages; superscript letters indicate significant differences within columns ($P < 0.05$).

less unsaturated FAs and tri-unsaturated TAGs, so its SFC curve was consistently below the other two curves. The SFC curve of AMF-B fell between those of AMF-A and AMF-C due to the mid-range content of its chemical composition.

The DSC studies provide an insight into the thermodynamics of fat phase transitions in AMFs (Fig. 2). A typical melting curve of AMF shows three endothermic peaks, corresponding to high, medium and low melting fractions. Their partial overlapping in the DSC experiment, which was strongly dependent on heating and cooling rates during the entire thermal history of the sample, reflects the occurrence of numerous thermal transitions (Lopez, Lesieur, Keller, & Ollivon, 2000). In this context, the melting and crystallisation temperatures of the AMF showed on the DSC curve were noteworthy with respect to the preparation of whipped cream since the formation of fat crystal play a key role in the texture and stability of whipped cream (Fredrick et al., 2013).

Fig. 2A illustrates the endothermic behaviour of AMFs. AMF-A had exhibited major endothermic progress by 38 °C and a broad melting range still with solid fat at 35 °C, whereas the other two AMFs possessed no solids at those temperatures (Fig. 1) and were void of endotherms at temperatures greater than 35 °C. AMF-B and AMF-C both exhibited their major endotherms at around 22–24 °C. All the AMFs contained some low-melting fat, as evidenced by the heat adsorption peaks at 6–8 and 12–14 °C. $\triangle H_M$ of AMF-A were considerably higher than those of AMF-B and AMF-C (Table 2). Compared with AMF-A, the other two samples were quite close in terms of the SFA contents (Table 1), which may have given rise to the higher similarity between the shape of their thermograms and their values of $\triangle H_M$.

Fig. 2B illustrates the DSC crystallisation exotherms for the AMFs obtained by cooling from 40 to −15 °C. The three AMFs presented similar exothermal curves during the cooling processing by showing sharp peaks at 14–16 °C and broad peaks at 6–7 °C. The exothermal curves had one peak less than those of the melting curves, in which three peaks were observed. This disparity reflects the diversity in the mechanisms of melting and crystallisation. The TAG has a variety of crystal forms. The sub-stable crystal first melts upon heating and the remaining TAG is then rearranged and recrystallised into a more stable form before, finally, melting at a higher temperature. This makes the melting process more complicated than the crystallisation process (Bootello et al., 2013). AMF-A crystallised at a slightly higher temperature compared with AMF-B and AMF-C, due to its higher SFA and S3 TAG content, which could crystallise independently of the bulk of the milk fat and return rapidly to the stable form (Lopez, Briard-Bion, Camier, & Gassi, 2006). Furthermore, AMF-A had a higher $\triangle H_C$ than both AMF-B and AMF-C (Table 2). According to the DSC profile, two major peaks appeared at around 7 and 15 °C for all three AMFs, as they were seen to undergo significant phase transitions and release a large amount of thermal energy near these two temperatures. This, therefore, suggests that these are the optimal two temperatures at which to whip RDCs and, as per the focus of this paper, to determine their whipping properties.

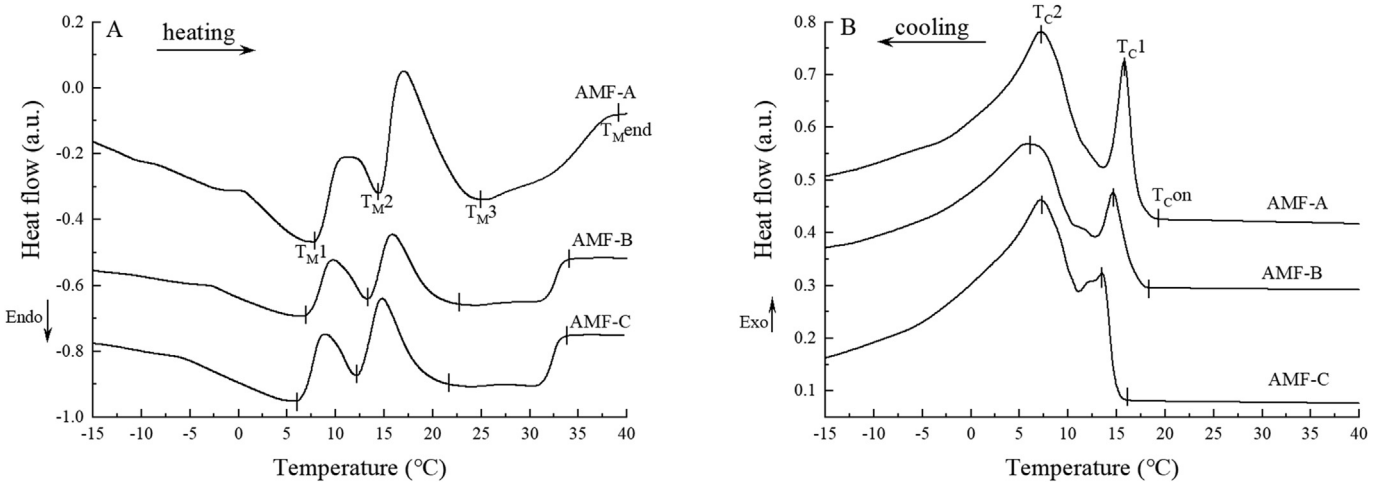

Fig. 2. Differential scanning calorimetric thermograms [(A) melting, (B) crystallisation] of anhydrous milk fats (AMF-A, AMF-B, AMF-C). T_{M1}, T_{M2} and T_{M3}: the melting point for the first, second and third peak; T_{Mend}: the final melting temperature (clarification temperature); $\triangle H_M$: enthalpy of melting; T_{Con}: the temperature of the beginning of crystallisation; T_{C1} and T_{C2}: the temperature of crystallisation for the first and second peak; $\triangle H_c$: enthalpy of crystallisation. Heat flow is given in arbitrary units (a.u.).

Table 2
Thermodynamic parameters for melting and crystallisation of different types of anhydrous milk fat (AMF).[a]

Samples	Melting					Crystallisation			
	T_{M1} (°C)	T_{M2} (°C)	T_{M3} (°C)	T_{Mend} (°C)	$\triangle H_M$ (J g^{-1})	T_{Con} (°C)	T_{C1} (°C)	T_{C2} (°C)	$\triangle H_C$ (J g^{-1})
AMF-A	7.84 ± 0.24	14.21 ± 0.14	25.30 ± 1.44	38.78 ± 0.74	59.65 ± 2.24	19.13 ± 0.14	15.72 ± 0.12	7.31 ± 0.32	12.85 ± 0.17
AMF-B	6.66 ± 0.19	13.36 ± 0.27	23.96 ± 1.35	34.13 ± 0.66	44.06 ± 1.18	18.24 ± 0.24	14.83 ± 0.23	6.03 ± 0.40	10.63 ± 0.22
AMF-C	6.03 ± 0.18	12.44 ± 0.26	23.15 ± 1.22	33.74 ± 0.46	41.38 ± 1.12	16.14 ± 0.16	13.36 ± 0.31	7.24 ± 0.42	9.93 ± 0.20

[a] Abbreviations are: T_{M1}, T_{M2} and T_{M3}, the melting point for the first, second and third peaks, respectively; T_{Mend}, the final melting temperature (clarification temperature); $\triangle H_M$, enthalpy of melting; T_{Con}, the temperature of the beginning of crystallisation; T_{C1} and T_{C2}, the temperature of crystallisation for the first and second peaks, respectively; $\triangle$Hc, enthalpy of crystallisation.

3.2. Crystallisation kinetics

In addition to equilibrium investigations, isothermal crystallisation curves can supply important clues to understand the crystallisation mechanism (Lopez, Lesieur, Bourgaux, Keller, & Ollivon, 2001). The isothermal crystallisation curves of the AMFs at different temperatures are shown in Fig. 3. All curves indicate two-step crystallisation, that is, a rapid increase followed by a plateau; however, the samples show curves of different shapes at 7 °C (Fig. 3A) and 15 °C (Fig. 3B), thus suggesting that there were different crystallisation mechanisms at play in the three AMFs. The AMFs crystallised rapidly at 7 °C and completed almost half of the crystallisation process in the first 3 min, with complete crystallisation within approximately 50 min. When isothermally crystallised at 15 °C, the crystallisation was only half completed after 20 min, but was completed after approximately 50 min, similarly to the process at 7 °C. Though the samples took a similar duration to complete the fat crystallisation process at the two temperatures, the extent of crystallisation at different temperatures was different. For each sample, its final content of SFC after crystallisation at 7 °C was at least 10% higher than that at 15 °C.

The most general model for the description of isothermal phase transformation is the Avrami equation. It is most prevalently used to evaluate crystallisation kinetics and unveil the nature of crystal growth. The Avrami parameters for the AMFs in this study, listed in Table 3, show a good fit of the kinetic data into the Avrami equation ($R^2 = 0.990–0.998$).

The crystallisation temperature exerted a significant influence on K values ($P < 0.05$), which were decreased by factors of 10 (for AMF-A) and 10^2 (for AMF-B and AMF-C) when the temperature increased from 7 °C to 15 °C, thus indicating that crystallisation proceeded slowly at the higher temperature due to lower nucleation and growth rate. A similar conclusion could be drawn from the variation in $t_{1/2}$, which increased from 7 °C to 15 °C and more directly reflected the slowdown of crystallisation. In comparison with AMF-A and AMF-C at the same crystallisation temperatures, AMF-A had higher K values and lower $t_{1/2}$ values ($P < 0.05$), indicating its stronger inclination towards crystallisation. In addition, n, a parameter in the Avrami equation used to indicate the dimensions of nucleation growth, was calculated and compared. According to the theory of Avrami equation, if n = 4, it suggests heterogeneous nucleation and spherulitic growth from sporadic nuclei; if n = 3, it suggests spherulitic growth, but from instantaneous nuclei; if n = 2, it represents high nucleation rate and plate-like growth, where growth is primarily along two dimensions; and if n = 1, it suggests that the nuclei are aggregated to form crystals instead of a linear growth (Herrera, Gatti, & Hartel, 1999). At 7 °C, the n values of all the samples were around 0.25. However, when the temperature increased to 15 °C, the n values varied from 1.0 (AMF-A) to 1.5 (AMF-C), thus indicating that a change in the type of nucleation and growth was induced by temperature. Specifically, a more rod-like growth around the instantaneous nuclei occurred at the lower temperature, while more plate-like growth around sporadic nuclei was seen at the higher temperature.

3.3. Emulsion stability

Generally, whipped cream is stored at 4 °C (Jakubczyk & Niranjan, 2006), so this temperature was used as a control in the stability analysis. The creaming stability of RDC prepared by the three AMFs at different temperatures (4, 7 and 15 °C) was compared. Fig. 4 displays the recorded evolution (from right to left) of time dependent transmission profiles for the RDCs. Creaming is

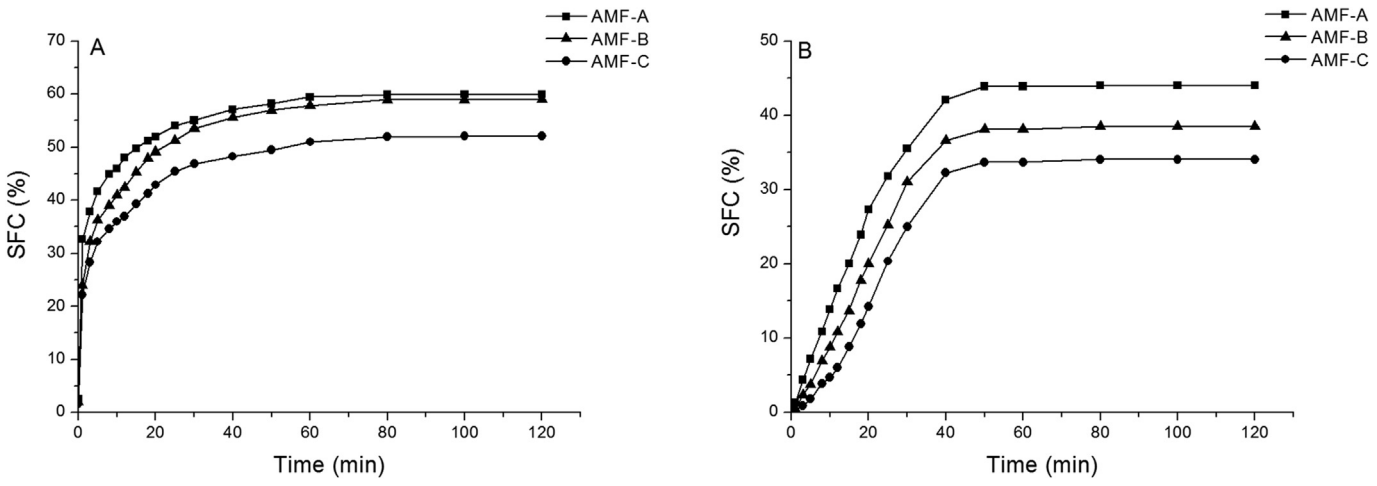

Fig. 3. Isothermal crystallisation curves of anhydrous milk fats at (A) 7 °C and (B) 15 °C: ■, AMF-A; ▲, AMF-B; ●, AMF-C.

Table 3
Avrami exponent (n), Avrami constant (K), and half-time of crystallisation ($t_{1/2}$) for anhydrous milk fat (AMF) crystals at 7 °C and 15 °C.[a]

Sample	Temperature (°C)	n	K (min^{-1})	$t_{1/2}$ (min)	R^2
AMF-A	7	0.205 ± 0.013	0.391 ± 0.013	16.293 ± 0.527	0.993
AMF-B	7	0.279 ± 0.007	0.283 ± 0.008	24.853 ± 0.761	0.990
AMF-C	7	0.256 ± 0.008	0.253 ± 0.002	51.824 ± 1.322	0.991
AMF-A	15	1.024 ± 0.035	0.014 ± 0.001	45.007 ± 1.425	0.998
AMF-B	15	1.223 ± 0.051	0.005 ± 0.001	51.593 ± 1.154	0.998
AMF-C	15	1.461 ± 0.063	0.002 ± 0.001	54.470 ± 1.074	0.998

[a] Values in each column (except for R^2) are significant different ($P < 0.05$).

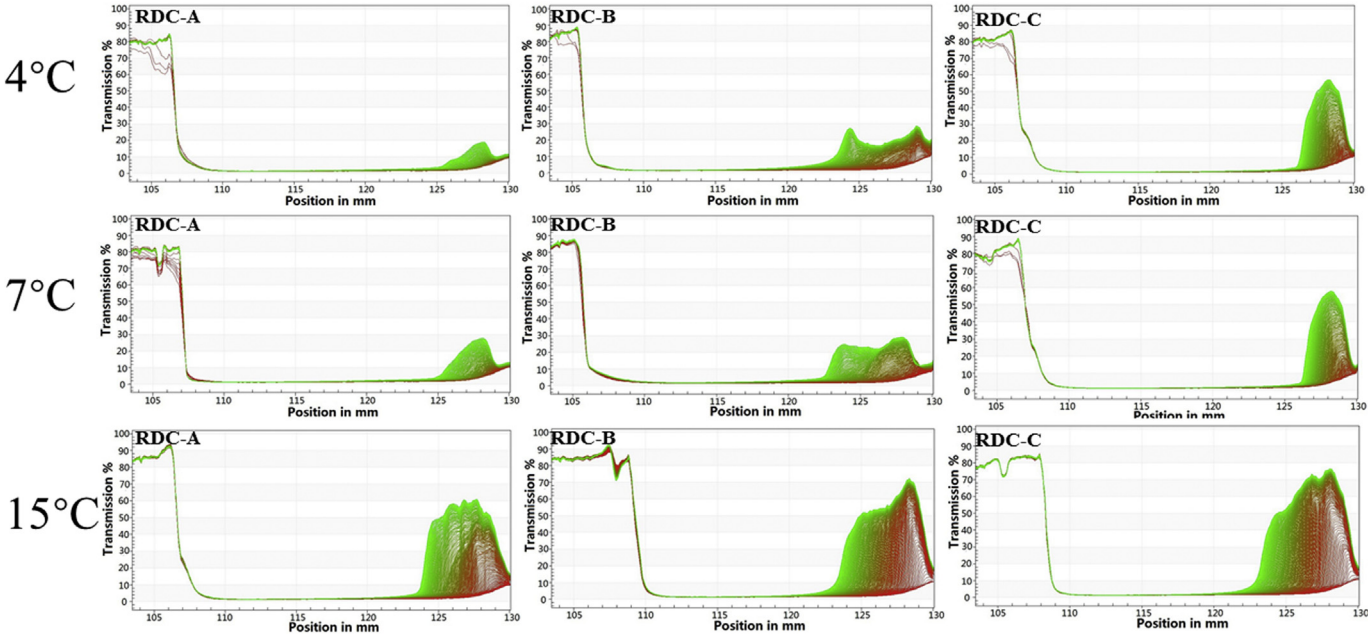

Fig. 4. Effect of temperature at 4 (A), 7 (B) and 15 °C (C) on the creaming stability of recombined dairy creams (RDCs). The slope of the integral transmission–time curve is an indicator of creaming stability. The initial transmission reading was presented by red line while the final transmission curve was in green. The curves between them, corresponding to each measurement, have gradual change in colours from red to green to show the measurement process. (For interpretation of the references to colour in this figure legend, the reader is referred to the Web version of this article.)

inevitable in almost all O/W emulsions, and can be greatly enhanced under centrifugation due to the difference in the mass density of dispersed oil phase and the continuous aqueous phase (Bigikocin et al., 2011). As shown in Fig. 4, in all the samples and at all three temperatures, NIR light was almost unable to pass through the upper position of the sample cell, which was occupied by accumulated fat content due to the centrifugation. The liquid-air phase boundary was found to be at 110 mm. The phase separation progressed in the direction from the bottom to the top of the cell. The overlay of profiles at the top of the RDC emulsion (from 120 to 130 mm) suggests that the complete separation has been achieved after centrifugation. As the test ran, centrifugation force separated the emulsion to two distinct phases progressively, i.e., the fat phase (toward the top of the sample cells) and aqueous phase (toward the bottom of the sample cells), which makes the transmission area at the bottom lager and more transparent (shown by ever-increasing transmission reading at the bottom). The transmission profile exhibited less change over space and time at lower temperatures (4 and 7 °C) compared with that at 15 °C, thus indicating better stability, while no significant difference was observed between these two lower temperatures. At the same temperature, RDC-A showed better stability compared with another two RDCs.

Two factors could have contributed to the high stability of RDC at 4 and 7 °C. First, variations in RDC particle size of the disperse phase may alter the crystallisation behaviour of AMFs and thus contribute to emulsion stability (Truong, Bansal, Sharma, Palmer, & Bhandari, 2014). The influences of temperature on the particle size distribution of RDC emulsions are depicted in Fig. 5. No significant difference was observed between 4 and 7 °C. The particle size distribution at lower temperature (4 and 7 °C) had a single peak in between 1 and 10 μm, whereas double peaks at 15 °C. The single peak in Fig. 5A,B suggested that the MFGs were distributed homogeneously and RDC emulsions were stable.

The second peak in Fig. 5C between 10 and 100 μm indicated the degree of MFG coalescence, RDC-C coalesced significantly than another two RDCs. In an emulsion system containing fat globules, when the temperature is at suitable low degree, fat crystals could form in the globules, and the fat crystals could protrude through the globule membrane to link the adjacent fat globules to some extent to construct a stable network (Thiel, Hartel, Spicer, & Hendrickson, 2016). As the temperature increased, fat crystals melted, and the fat globules tended to merge together driven by Laplace pressure to create larger spherical droplets to minimise the interfacial area, and further merging would form large flocculation of fat content (Le, Camp, Rombaut, Leeckwyck, & Dewettinck,

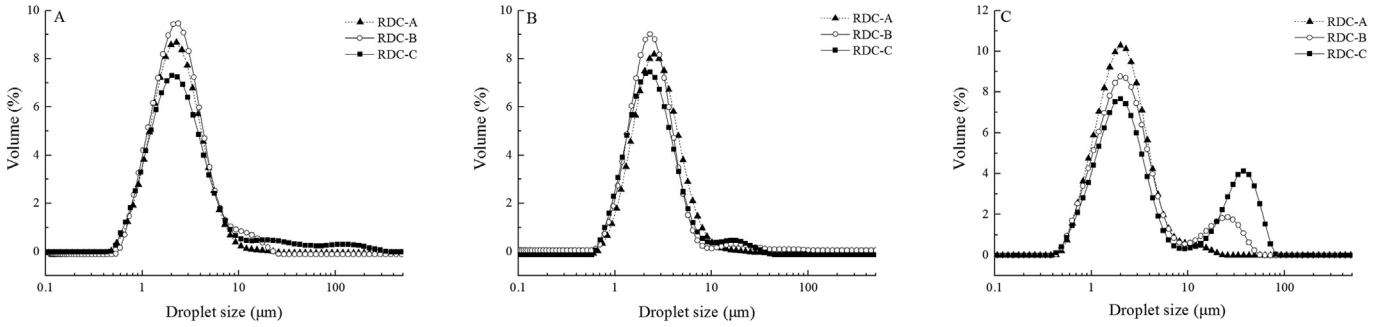

Fig. 5. Effect of temperature at (A) 4, (B) 7 and (C) 15 °C on the particle size distribution of recombined dairy creams (▲, RDC-A; ○, RDC-B; ■, RDC-C).

2009). Increasing the temperature from 4 to 15 °C decreased the SFC by nearly half in all AMF samples and the SFC at 15 °C of RDC-C was the least (Fig. 1), which means at lower temperature, crystals could move energetically to a more favourable interface, where they project into the adjacent MFGs and wet them to form a strong network, thus increasing the partial coalescence efficiency (Ronholt, Kirkensgaard, Pedersen, Mortensen, & Knudsen, 2012). However, higher temperature could lead to melt of fat, which signifies less SFC and less crystallised fat and further causes the collapse of previously formed partial coalescence structure or impede the formation of this structure. The MFGs with less partial coalescence structure are less stable and easily cause creaming during centrifugation operation.

3.4. Whipping properties

Table 4 lists the whipping properties of the RDC whipped at 4, 7 and 15 °C. The optimum whipping time (t_{wh}) is a useful criterion in evaluating partial coalescence of dairy cream. Hotrum et al. (2005) suggests that a shorter t_{wh} provides evidence of an increase in surface-mediated partial coalescence at an air or water interface in cream.

According to Table 4, for each of the RDCs, all of its three parameters showed no significant difference with temperature increasing from 4 to 7 °C ($P > 0.05$); however, with further increases of temperature up to 15 °C, the t_{wh} significantly increased, while overrun (OR) and firmness significantly decreased ($P < 0.05$). OR is one of the most effective parameters affecting the textural properties and stability of whipped cream. The comparison between the three samples showed that RDC-A yielded lowest OR. Higher foam firmness indicates higher foam stability, which helps to achieve higher OR values. The OR of whipped cream depends not only on the protein concentration of the serum phase, but also on the speed and extent of the partial coalescence of fat (Zhao et al., 2013). Partial coalescence at a lower temperature, of 4 or 7 °C compared with 15 °C, contributes to a better network of fat globules which traps a large amount of air bubbles. Here, as the temperature rose, the crystals melted and the network of fat globules tended to collapse (Fig. 6), thus decreasing the ability to trap air bubbles.

Table 4
Whipping properties of recombined dairy creams (RDCs) prepared by different kinds of anhydrous milk fat at 4, 7 and 15 °C.[a]

Sample	Temperature (°C)	t_{wh} (min)	Overrun (%)	Firmness (N)
RDC-A	4	3.28 ± 0.21^{a}	125.05 ± 1.10^{a}	70.27 ± 1.20^{a}
RDC-B	4	4.68 ± 0.18^{b}	140.62 ± 2.80^{b}	54.55 ± 3.12^{b}
RDC-C	4	5.13 ± 0.10^{c}	132.97 ± 2.45^{c}	46.14 ± 2.58^{c}
RDC-A	7	3.40 ± 0.11^{a}	124.05 ± 1.00^{a}	67.27 ± 2.30^{a}
RDC-B	7	4.76 ± 0.15^{b}	144.12 ± 3.20^{b}	55.87 ± 3.42^{b}
RDC-C	7	5.02 ± 0.20^{c}	136.67 ± 2.01^{c}	44.78 ± 3.51^{c}
RDC-A	15	4.56 ± 0.22^{d}	108.81 ± 0.80^{d}	50.14 ± 1.21^{d}
RDC-B	15	5.47 ± 0.14^{e}	115.78 ± 1.51^{e}	32.78 ± 1.50^{e}
RDC-C	15	6.02 ± 0.42^{f}	122.09 ± 1.12^{f}	29.98 ± 2.10^{f}

[a] t_{wh} is the optimum whipping time; superscript letters within columns indicate significant differences ($P < 0.05$).

The fat globule collapse of RDC-B and RDC-C can be seen from the increase of flocculation of MFGs, broken air bubbles and uncovered bubbles at 15 °C. Furthermore, for each of the RDC samples, it showed equal values of firmness ($P > 0.05$) at 4 and 7 °C, which were much higher than the value at 15 °C, and at each temperature, the firmness of the samples followed a sequence of RDC-A > RDC-B > RDC-C (Table 4). The considerable decrease in these parameters suggests a signal for the structural collapse of the RDC. These results thus confirm that whipping at 15 °C is not constructive for the formation of partially coalesced MFGs, for which an appropriate ratio between fat crystal and fat liquid is required (Börjesson, Dejmek, Löfgren, Paulsson, & Glantz, 2015; Moens et al., 2016).

3.5. Microstructure

The correlation between the DSC, SFC and their different nucleation and growth mechanisms at different temperatures of AMFs, together with the whipping properties of the RDCs, imply differences in the crystal morphologies of the three AMFs and the quality of the corresponding RDCs. CLSM, the most popular method to visualise the microstructure of whipped cream (Fredrick et al., 2013), was employed to observe the RDCs, as shown in Fig. 6. The distinct foam structure created by whipping is the result of the balance between the partial coalescence of MFGs and air bubbles (Moens et al., 2016). Here, big clumps of MFGs occurred at both the air bubble surfaces and in the serum phase, observed in the micrographs as intense red regions. The black air bubbles were covered with protein dyed by green fluorescent pigment.

No differences were observed between the graphs at 4 and 7 °C for all the RDC. Air bubbles were almost wrapped by proteins and MFGs were partially coalesced in the serum phase due to linking fat crystals. All whipped RDCs had air bubbles of a spherical shape, and the MFGs were small and well-distributed to form a MFG network. It was more obvious that, at the lower temperatures, RDC-A produced spherulites of large MFGs, which were dense and close to each other, however, at the higher temperature, the spherulites became smaller. Hence, these images clearly show that the degree of partially coalesced MFGs, both at the air bubble surface and in the serum phase, increases at lower temperatures and decreases at higher temperatures. The SFCs at both 4 and 7 °C were higher than those at 15 °C (Fig. 1), suggesting that the stability of air bubbles could increase at a lower whipping temperature, due to the network structure harbouring more solid crystals. About 65–75% of the crystalline fat melted at 15 °C (Fig. 1), making the crystalline network skeleton insufficient to support the foam structure. In this

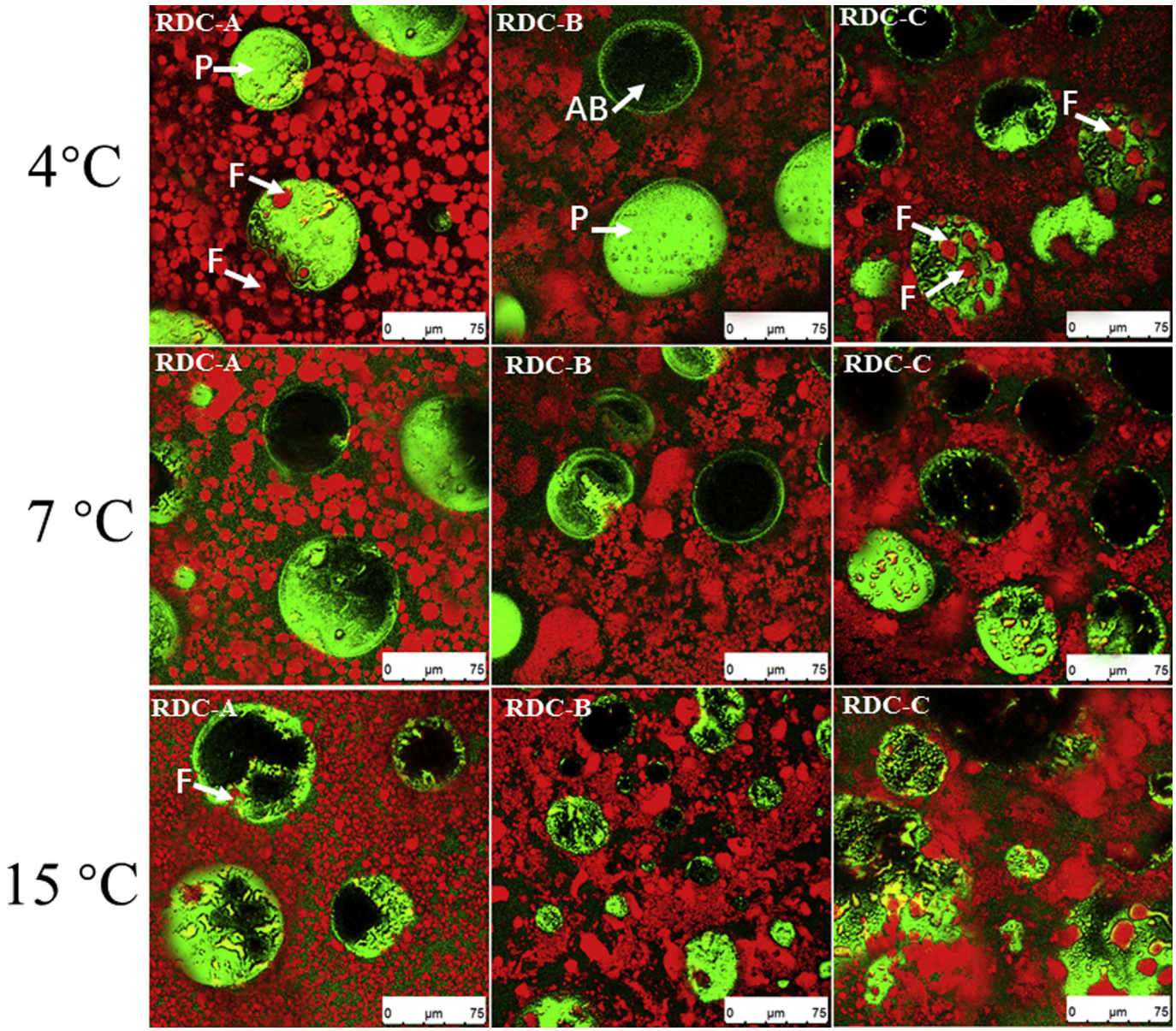

Fig. 6. Confocal laser scanning microscopy (CLSM)-micrographs of whipped dairy cream at 4, 7 and 15 °C. Protein is marked by green, and fat is marked by red. The circle area marked by a green surface or a green circle edge with black inner are air bubbles. Green circles and area indicate protein membranes. (For interpretation of the references to colour in this figure legend, the reader is referred to the Web version of this article.)

state, the fat crystals network is structurally weak, so that even slight agitation may lead to its dismemberment.

However, a significant difference was observed in the distribution of MFGs and the state of the wrapped air bubbles in different RDCs at the same temperature. At 4 and 7 °C, MFGs in RDC-A were more homogeneously distributed with smaller sizes and more regular shapes in comparison to RDC-B and RDC-C, which were observed with irregular flocculation (in RDC-B) or aggregation (in RDC-C) of MFGs. Moreover, in RDC-C, the air bubble surfaces were covered with more MFGs than the other two RDCs, which should, in the serum phase, form a stable network. When whipped at 15 °C, flocculation and broken air bubbles were significantly increased for RDC-C. In RDC-B, only a few small bubbles covered with MFGs could be detected. By contrast, the microstructure of RDC-A showed few distinct changes with the variation in temperature. This may be attributed to the higher number of S3 TAG in AMF-A, which means AMF-A has higher saturation and melting points, which enable it to achieve a stiffer crystal network (Table 1). A more rigid RDC-A system is in accordance with the higher SFC shown in Fig. 1. As a W/O emulsion, whipped cream is heterogeneous at a microscopic level, consisting of a finely divided water phase and a continuous phase comprising fat crystals and liquid oil. During the manufacture of the pre-emulsion and its crystallisation upon cooling, the fat globules present in the overwhelming continuous phase rapidly adsorb to the W/O interfaces, according to the well-known Pickering stabilising mechanism (Kim, Bot, de Vries, Golding, & Pelan, 2013).

4. Conclusion

This study enhances the knowledge about the effect of temperatures on the whipping properties and stability of RDC. It determined that DSC is an effective tool for ascertaining the most suitable whipping temperature to yield whipped dairy cream of higher quality. The results discover that, in comparison to a higher

temperature, better stability, shorter t_{wh}, higher OR and better firmness of RDCs are achieved by lower temperatures at 4 and 7 °C, a temperature variation between which shows no significant influence on these parameters. From an energy-saving perspective, it therefore makes sense to select 7 °C as the optimum temperature at which to store and whip RDC. It is worth noting that, as milk fat crystallisation was found in this study to play an important role in RDC quality, future research is suggested to unveil the SFC, crystallisation kinetics and thermodynamics of the individual components of AMF to gain a more complete profile of whipped dairy cream.

Acknowledgements

This work was supported by the The National Dairy Industry and Technology System of China (grant no. CARS-36) and Beijing Postdoctoral Research Foundation (2018-ZZ-010).

References

Bigikocin, E., Mert, B., & Alpas, H. (2011). Effect of high hydrostatic pressure and high dynamic pressure on stability and rheological properties of model oil-in-water emulsions. *High Pressure Research, 31*, 462–474.

Bootello, M. A., Hartel, R. W., Levin, M., Martínez-Blanes, J. M., Real, C., Garcés, R., et al. (2013). Studies of isothermal crystallisation kinetics of sunflower hard stearin-based confectionery fats. *Food Chemistry, 139*, 184–195.

Börjesson, J., Dejmek, P., Löfgren, R., Paulsson, M., & Glantz, M. (2015). The influence of serum phase on the whipping time of unhomogenised cream. *International Dairy Journal, 49*, 56–61.

Drelon, N., Gravier, E., Daheron, L., Boisserie, L., Omari, A., & Leal-Calderon, F. (2006). Influence of tempering on the mechanical properties of whipped dairy creams. *International Dairy Journal, 16*, 1454–1463.

Fredrick, E., Heyman, B., Moens, K., Fischer, S., Verwijlen, T., Moldenaers, P., et al. (2013). Monoacylglycerols in dairy recombined cream: II. The effect on partial coalescence and whipping properties. *Food Research International, 51*, 936–945.

Fredrick, E., Walstra, P., & Dewettinck, K. (2010). Factors governing partial coalescence in oil-in-water emulsions. *Advances in Colloid and Interface Science, 153*, 30–42.

Han, J., Zhou, X., Cao, J., Wang, Y., Sun, B., Li, Y., et al. (2018). Microstructural evolution of whipped cream in whipping process observed by confocal laser scanning microscopy. *International Journal of Food Properties, 21*, 593–605.

Herrera, M. L., de Leon Gatti, M., & Hartel, R. W. (1999). A kinetic analysis of crystallization of a milk fat model system. *Food Research International, 32*, 289–298.

Hotrum, N. E., Stuart, M. A. C., van Vliet, T., Avino, S. F., & van Aken, G. A. (2005). Elucidating the relationship between the spreading coefficient, surface-mediated partial coalescence and the whipping time of artificial cream. *Colloids and Surfaces A: Physicochemical and Engineering Aspects, 260*, 71–78.

Jakubczyk, E., & Niranjan, K. (2006). Transient development of whipped cream properties. *Journal of Food Engineering, 77*, 79–83.

Kamath, S., Huppertz, T., Houlihan, A. V., & Deeth, H. C. (2008). The influence of temperature on the foaming of milk. *International Dairy Journal, 18*, 994–1002.

Karabulut, I., Turan, S., & Ergin, G. (2004). Effects of chemical interesterification on solid fat content and slip melting point of fat/oil blends. *European Food Research and Technology, 218*, 224–229.

Kim, H. J., Bot, A., de Vries, I. C. M., Golding, M., & Pelan, E. G. (2013). Effects of emulsifiers on vegetable-fat based aerated emulsions with interfacial rheological contributions. *Food Research International, 53*, 342–351.

Le, T. T., Camp, J. V., Rombaut, R., Leeckwyck, F. V., & Dewettinck, K. (2009). Effect of washing conditions on the recovery of milk fat globule membrane proteins during the isolation of milk fat globule membrane from milk. *Journal of Dairy Science, 92*, 3592–3603.

Liu, Y., Meng, Z., Zhang, F., Shan, L., & Wang, X. (2010). Influence of lipid composition, crystallization behavior and microstructure on hardness of palm oil-based margarines. *European Food Research and Technology, 230*, 759–767.

Lopez, C., Briard-Bion, V., Camier, B., & Gassi, J.-Y. (2006). Milk fat thermal properties and solid fat content in Emmental cheese: A differential scanning calorimetry study. *Journal of Dairy Science, 89*, 2894–2910.

Lopez, C., Lesieur, P., Bourgaux, C., Keller, G., & Ollivon, M. (2001). Thermal and structural behavior of milk fat: 2. Crystalline forms obtained by slow cooling of cream. *Journal of Colloid and Interface Science, 240*, 150–161.

Lopez, C., Lesieur, P., Keller, G., & Ollivon, M. (2000). Thermal and structural behavior of milk fat: 1. Unstable species of cream. *Journal of Colloid and Interface Science, 229*, 62–71.

Moens, K., De Clercq, N., Verstringe, S., & Dewettinck, K. (2015). Revealing the Influence of tempering on polymorphism and crystal arrangement in semi-crystalline oil-in-water emulsions. *Crystal Growth & Design, 15*, 5693–5704.

Moens, K., Masum, A. K. M., & Dewettinck, K. (2016). Tempering of dairy emulsions: Partial coalescence and whipping properties. *International Dairy Journal, 56*, 92–100.

Meng, Z., Liu, Y. F., Jin, Q. Z., Huang, J. H., Song, Z. H., Wang, F. Y., et al. (2011). Comparative Analysis of Lipid Composition and Thermal, Polymorphic, and Crystallization Behaviors of Granular Crystals Formed in Beef Tallow and Palm Oil. *Journal of Agricultural and Food Chemistry, 59*, 1432–1441.

Ronholt, S., Kirkensgaard, J. J., Pedersen, T. B., Mortensen, K., & Knudsen, J. C. (2012). Polymorphism, microstructure and rheology of butter. Effects of cream heat treatment. *Food Chemistry, 135*, 1730–1739.

Sajedi, M., Nasirpour, A., Keramat, J., & Desobry, S. (2014). Effect of modified whey protein concentrate on physical properties and stability of whipped cream. *Food Hydrocolloids, 36*, 93–101.

Smith, A. K., Go, H. D., & Kakuda, Y. (2000). Microstructure and rheological properties of whipped cream as affected by heat treatment and addition of stabilizer. *International Dairy Journal, 10*, 295–301.

Thiel, A. E., Hartel, R. W., Spicer, P. T., & Hendrickson, K. J. (2016). Coalescence behavior of pure and natural fat droplets characterized via micromanipulation. *Journal of the American Oil Chemists' Society, 93*, 1467–1477.

Tomaszewska-Gras, J. (2013). Melting and crystallization DSC profiles of milk fat depending on selected factors. *Journal of Thermal Analysis and Calorimetry, 113*, 199–208.

Truong, T., Bansal, N., Sharma, R., Palmer, M., & Bhandari, B. (2014). Effects of emulsion droplet sizes on the crystallisation of milk fat. *Food Chemistry, 145*, 725–735.

Wang, F., Liu, Y., Jin, Q., Huang, J., Meng, Z., & Wang, X. (2011). Kinetic analysis of isothermal crystallization in hydrogenated palm kernel stearin with emulsifier mixtures. *Food Research International, 44*, 3021–3025.

Yuan, F., Xu, D., Qi, X., Zhao, J., & Gao, Y. (2011). Impact of high hydrostatic pressure on the emulsifying properties of whey protein isolate–chitosan mixtures. *Food and Bioprocess Technology, 6*, 1024–1031.

Zhao, Q., Kuang, W., Long, Z., Fang, M., Liu, D., Yang, B., et al. (2013). Effect of sorbitan monostearate on the physical characteristics and whipping properties of whipped cream. *Food Chemistry, 141*, 1834–1840.

Zhou, X., Chen, L., Han, J., Shi, M., Wang, Y., Zhang, L., et al. (2016). Stability and physical properties of recombined dairy cream: Effects of soybean lecithin. *International Journal of Food Properties, 20*, 2223–2233.